

1. Introduction

Active regions (ARs) are locations in the Sun's atmosphere of enhanced magnetic field, observed as bright hot ($>1\text{MK}$) loops in extreme ultraviolet (EUV) and soft X-rays (SXR). The precise details of the mechanism to heat this material are still debated; one idea is of small impulsive releases of energy (liberated from the magnetic field) to heat the material, sometimes referred to as "nanoflares". ARs are the source of large flares (GOES X-Class) down to microflares ($< \text{GOES A,B-Class}$) in which energy is rapidly released to accelerate particles and heat material but the connection to smaller more frequent "nanoflares" is still uncertain. We need to carefully investigate the smallest microflares as well as ARs that do not appear to be flaring (yet are still hot) to see whether an ensemble of "nano" events is possible (Klimchuk, 2015).

We present a preliminary study of the heating in AR12333 due to small microflares between 10:30 and 13:30UT on 29 April 2015. This region is well observed in EUV with the Atmospheric Imaging Assembly (AIA) on board the *Solar Dynamics Observatory* (SDO) and *Hinode's* X-ray Telescope, XRT. The latter were a coordinated campaign with the *NuSTAR* hard X-ray focusing optics telescope (Harrison *et al.* 2013). The *NuSTAR* data for AR12333 is at a very early stage of analysis so this poster will focus on the thermal characteristics of AR12333 from the SDO/AIA and *Hinode*/XRT data at the times of combined observations (11:30 and 13:00UT).

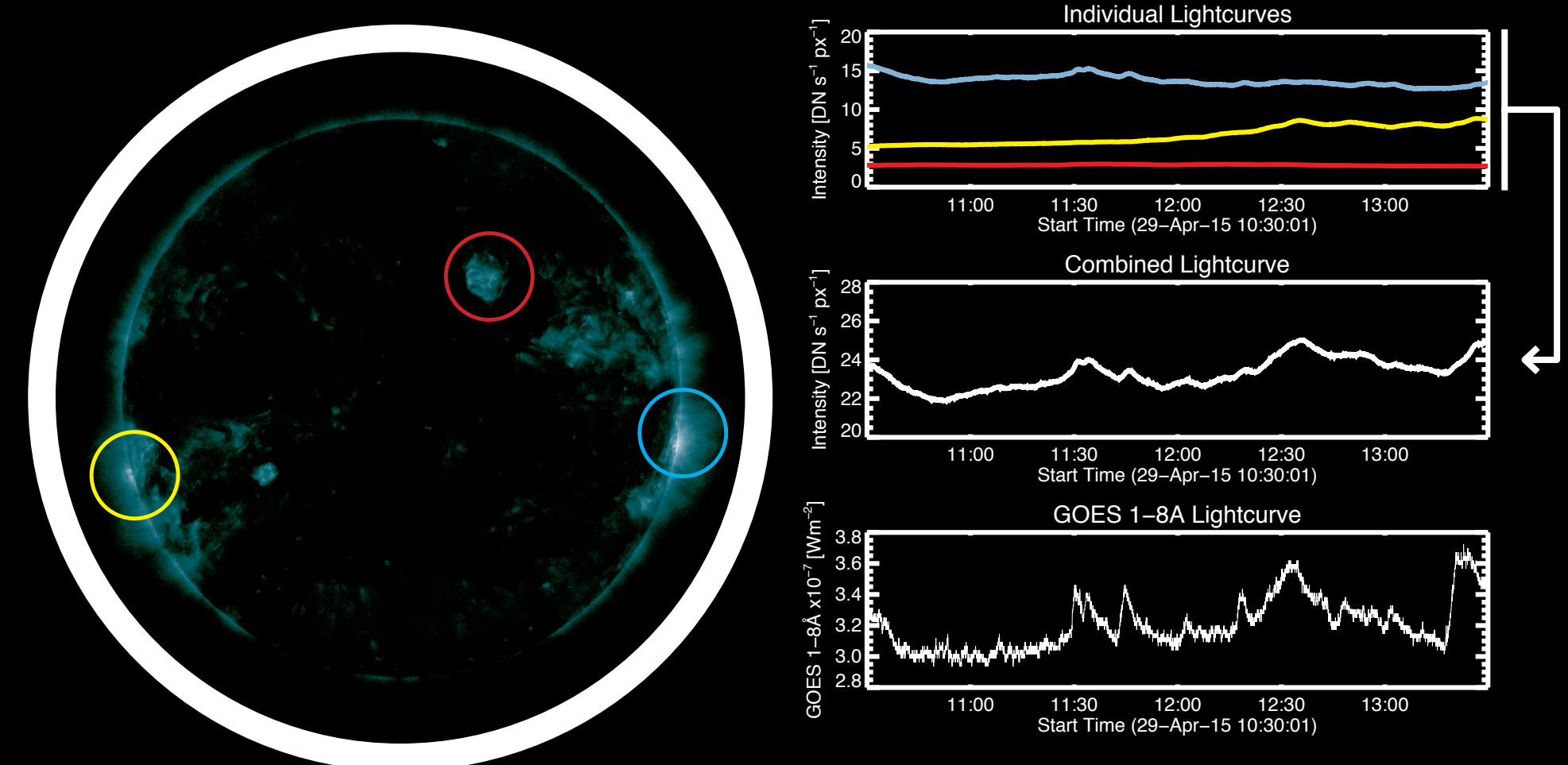


Figure 1: Left: SDO/AIA 94Å observation at 11:30UT showing three flaring regions; AR12333 is indicated by a red circle. Right: Individual lightcurves in SDO/AIA 94Å of the three regions (top), and a combined lightcurve of all regions (middle) matching the features of the GOES 1-8Å lightcurve (bottom). The two limb regions (yellow and blue) are responsible for the B-class microflares observed in GOES.

2. Data and Analysis

The solar activity during the time of the combined *NuSTAR* and *Hinode*/XRT observations is shown in figure 1 with AR12333 highlighted by the red circle. AR12333 is not the brightest on the disk with the two other regions producing B-class microflares during the time period (10:30 to 13:30UT) as seen by the 94Å lightcurve – the microflares in AR12333 must be below B-level.

The evolution of AR12333 can be seen using *Hinode*/XRT Be-Thin filter images in figure 2 (below) – with those at 11:30 and

References:

- Del Zanna 2013, *A&A*, 558, A73
Dere *et al.* 1997 *A&A Supp. Series*, 125, 149
Hannah & Kontar 2012, *A&A*, 539, A146
Hannah & Kontar 2013, *A&A*, 553, A10
Harrison *et al.* 2013 *ApJ*, 770, 103
Klimchuk 2015, *Phil. Trans. R. Soc. A*, 373, 2042
Kobelski *et al.* 2013, *Sol. Phys.*, 289, 2781
Landi *et al.* 2013, *ApJ*, 763, 86
Narukage *et al.* 2014, *Sol. Phys.*, 289, 1029

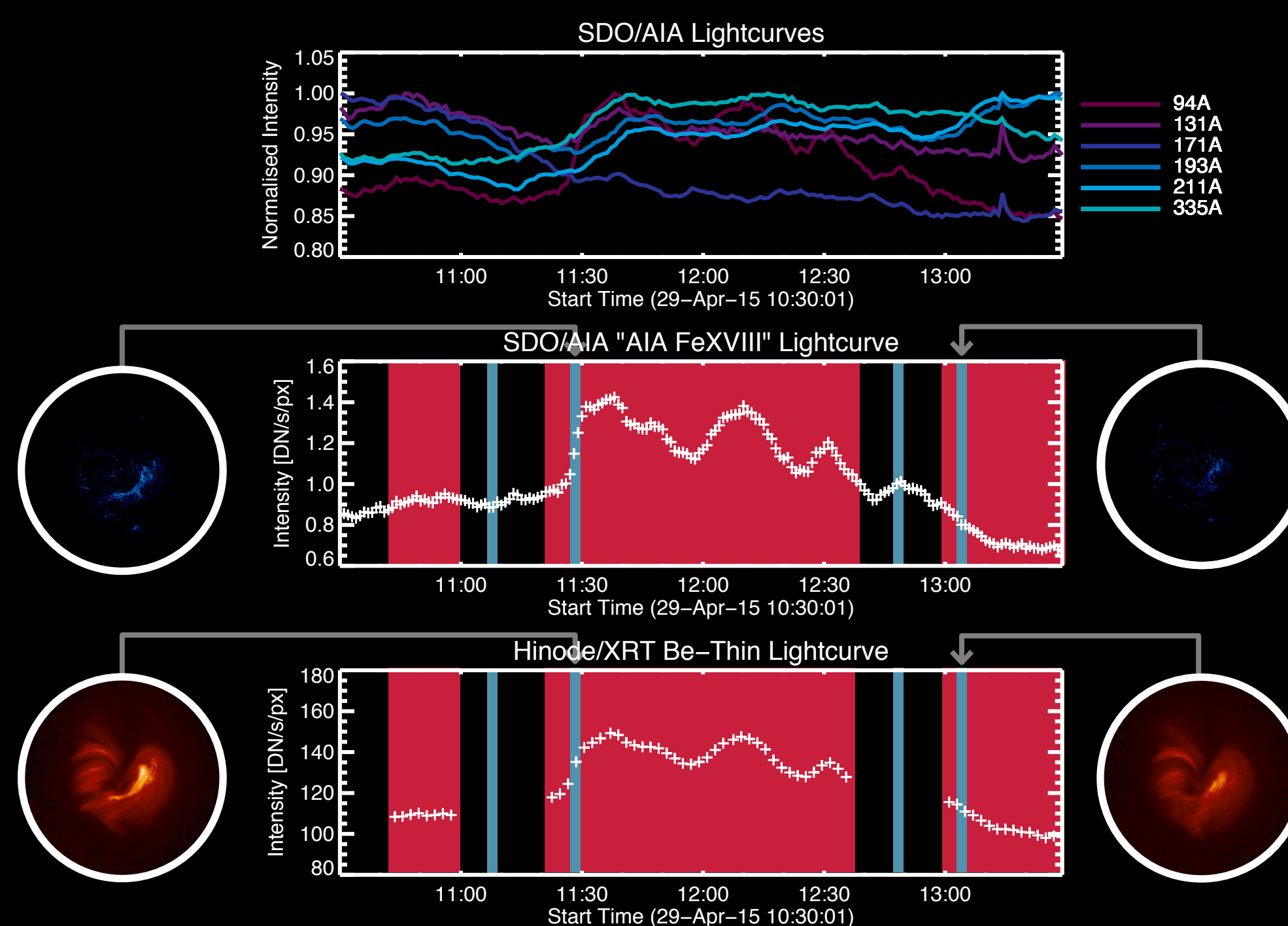


Figure 3: SDO/AIA, SDO/AIA Fe XVIII, and *Hinode*/XRT Be-Thin lightcurves with the time periods of *Hinode*/XRT observations in red, and *NuSTAR* observations, blue for the latter two subfigures. Top: SDO/AIA lightcurves for AR12333. Middle: SDO/AIA Fe XVIII lightcurve for AR12333. Bottom: *Hinode*/XRT Be-Thin lightcurve for AR12333. Additionally, SDO/AIA Fe XVIII images and *Hinode*/XRT Be-Thin images are shown at the times of synchronous *Hinode*/XRT and *NuSTAR* observations (11:30 and 13:00UT).

13:00 being synchronous observations with *NuSTAR* – and the bottom panel of figure 3. Figure 2 shows the microflares heating a main arc of coronal loops before cooling back down, and figure 3 (bottom panel) shows the associated lightcurve of the loop region. Given the gaps in *Hinode*/XRT observations we also show the SDO/AIA lightcurves (top panel). We observe some similar variation to that in *Hinode*/XRT Be-Thin predominantly in the 94Å channel, and have isolated the hot Fe XVIII component from the 94Å lightcurve (middle panel; see Del Zanna 2013).

To recover the amount of material as a function of temperature from the SDO/AIA and *Hinode*/XRT data we determine the Differential Emission Measure (DEM) using the regularized inversion method of Hannah and Kontar 2012, 2013. The input is the temperature response for each of the filters on SDO/AIA (calculated using CHIANTI; Dere *et al.* 1997, Landi *et al.* 2013) and *Hinode*/XRT (using APEC), and the emission for the the same loop region per filter channel; the temperature responses can be seen in figure 4. We note there is unknown organic contamination present on the *Hinode*/XRT CCD, opaque to longer wavelength X-rays that are generally admitted by the thinner filters (Kobelski *et al.* 2013, Narukage *et al.* 2014). In this analysis we include the affected pixels, but do not include observations from the thinnest filters.

The resulting DEMs are shown in figure 5 for both 11:30 and 13:00UT. Given the uncertainties and difficulties in robustly recovering DEMs we have tried different combinations of the data available to reconstruct the underlying DEM. In general there are two broad components – one about 1MK (the ambient corona/AR) and another 10MK (likely due to the microflares).

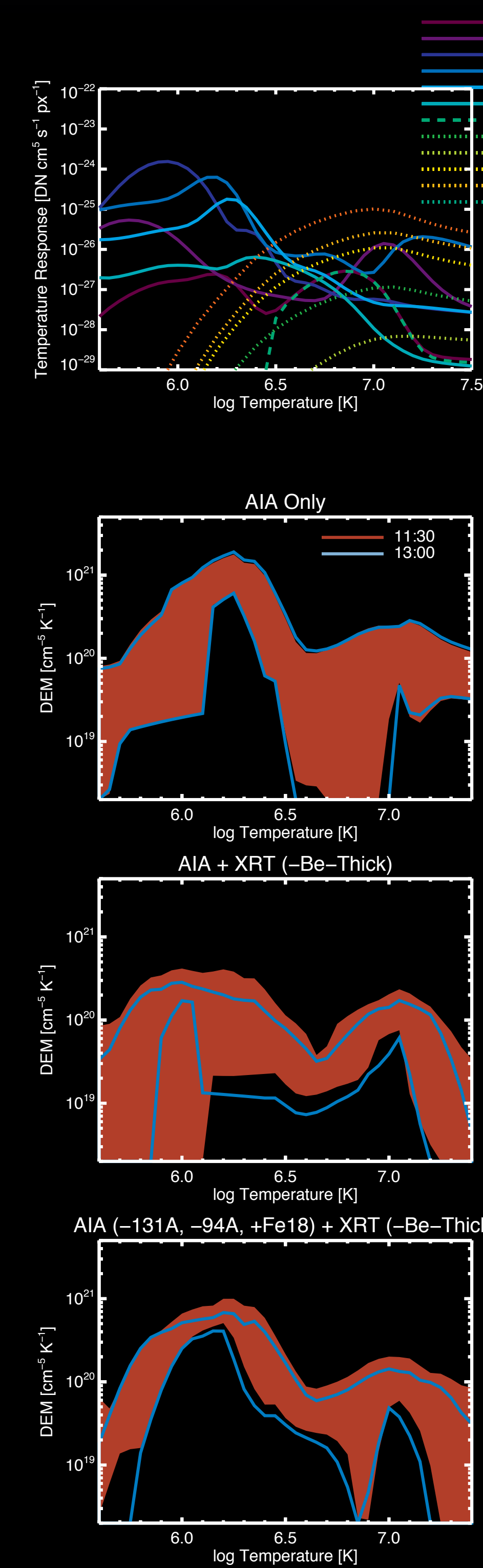


Figure 4: Temperature response curves for the 6 SDO/AIA filter channels and the 5 *Hinode*/XRT filter channels. SDO/AIA filter channels are represented by solid lines; SDO/AIA Fe XVIII, dashed line; *Hinode*/XRT, dotted lines.

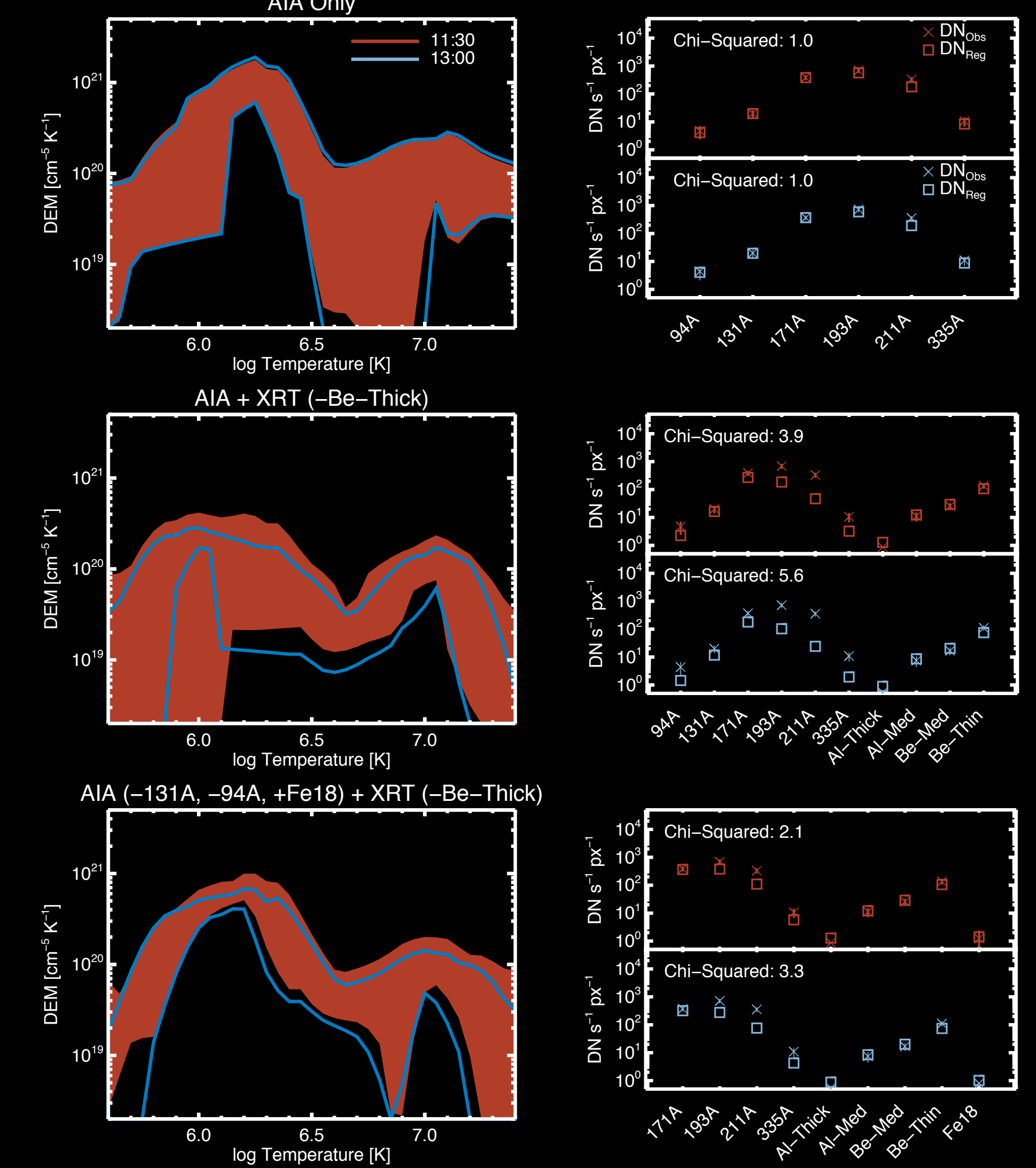


Figure 5: Left column: DEM for varying filter combinations with the red region indicating the DEM at 11:30, and the blue region indicating the DEM at 13:00: 6 SDO/AIA channels only, 6 from SDO/AIA combined with 4 *Hinode*/XRT, and the combination of 4 SDO/AIA filters and the Fe XVIII component of SDO/AIA 94Å combined with 4 *Hinode*/XRT filters. Right column: Observed (from images) and simulated data (from the DEM) for each filter.

3. Summary

- We have shown the preliminary analysis of microflares in AR12333 observed with SDO/AIA and *Hinode*/XRT, and recovered the DEMs of the whole brightening loop regions at two intervals synchronous with *NuSTAR* observations.
- DEMs show a variety of behaviour and future work is required to find the optimal combination of SDO/AIA and *Hinode*/XRT filters.
- We will have the *NuSTAR* derived thermal properties to help constrain the DEM further, but this is at a time of high solar emission (figure 1) and thus the temperature constraints may be limited.
- We will investigate the spatial and temporal evolution of AR12333 in detail.
- We will also compare the time evolution to AR/loop heating models.

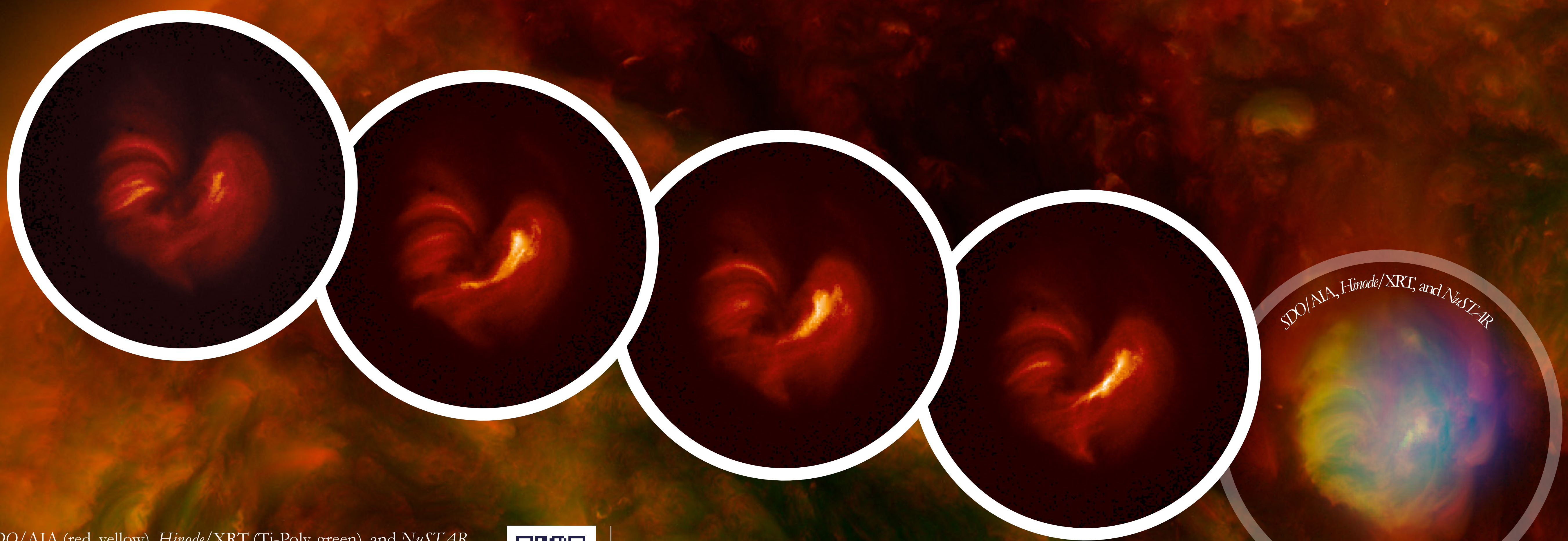


Figure 2: A SDO/AIA (red, yellow), *Hinode*/XRT (Ti-Poly, green), and *NuSTAR* (blue) composite with overlying *Hinode*/XRT Be-Thin filter images (scaled identically) showing the heating and cooling of an arc of loops from 11:00 to 13:00UT. Synchronous *NuSTAR* observations are present at 11:30 and 13:00UT.

